

A new well-posed nonlocal Perona-Malik type equation

PATRICK GUIDOTTI

Abstract

A modification of the Perona-Malik equation is proposed for which the local nonlinear diffusion term is replaced by a nonlocal term of slightly reduced “strength”. The new equation is globally well-posed (in spaces of classical regularity) and possesses desirable properties from the perspective of image processing. It admits characteristic functions as (formally linearly “stable”) stationary solutions and can therefore be reliably employed for denoising keeping blurring in check. Its numerical implementation is stable, enhances some of the features of Perona-Malik, and avoids problems known to affect the latter.

1. Introduction

The Perona-Malik equation [14]

$$u_t - \operatorname{div}\left(\frac{1}{1 + |\nabla u|^2} \nabla u\right) = 0 \quad (1.1)$$

on a domain $\Omega \stackrel{\circ}{\subset} \mathbb{R}^n$ is usually complemented with homogeneous Neumann boundary conditions. The nonlinear diffusion coefficient

$$a(u) = \frac{1}{1 + |\nabla u|^2}$$

is sometimes replaced by $a(u) = e^{-|\nabla u|^2}$. Perona and Malik originally introduced (1.1) in the context of image processing with the aim of denoising a given image u_0 while at the same time controlling blurring. The latter is unavoidable if a linear diffusion equation is used instead. The nonlinear diffusion determined by $a(u)$ significantly impedes diffusion in directions of

steep gradients which correspond to sharp edges in the image. If one considers a large gradient across a surface, then the nonlinear diffusion coefficient leads to diffusion in tangential directions and backward diffusion in normal direction. This is the reason why models of this type are often referred to as anisotropic diffusion models.

Numerical approximations of (1.1) have confirmed this prediction and have been successfully employed as a consequence. It has, however, been observed that discretizations of (1.1) often lead to stair-casing in the numerical solution (see Figure 1), or, more in general, to the preservation of gradients which do not represent any image feature but might simply be due to the presence of noise (cf. [14, 1] and Figure 4). Equation (1.1) poses many a challenge from the analytical point of view. It is an example of so-called forward-backward diffusion. In [10] the author shows that it is not well-posed. To circumvent this problem a variety of regularization techniques have been proposed. Spatial regularizations were the first to appear in [6, 1]. The gain in analytical tractability is, however, offset by the introduction of blurring. Temporal and spatio-temporal regularizations have also been considered, see [12, 8, 7, 4, 5, 2]. In [2] the author considers a purely temporal regularization which leads to time-delayed Perona-Malik equation which mimics the implicit linearization procedure common to all numerical discretizations of (1.1), that is

$$\begin{cases} u^{n+1} = u^n + \operatorname{div}(a(u^n)\nabla u^{n+1})\delta t & n \geq 0, \\ u^0 = u_0 & n = 0, \end{cases}$$

whereby the nonlinearity is always evaluated at the previous time step. The introduction of a time delay leads to a tractable analytical problem and does not seem to negatively impact the desired features of a corresponding numerical implementation. The author proves local existence of a regular solution for the delay equation.

Variational techniques have also been utilized to gain analytical understanding of (1.1) in a one-dimensional context. The Perona-Malik equation can in fact be viewed as the gradient flow associated with the non-convex energy functional

$$E(u) = \int_0^1 \log(1 + |\nabla u|^2), \quad u \in H^1(\Omega).$$

Using concepts and techniques related to Young-measure solutions various results have been obtained. [15, 16] prove instability of certain solutions and the existence of infinitely many solutions of a certain (weak) type.

Equation (1.1) was motivated by its potential applications to image processing. Whereas it poses significant and interesting mathematical challenges, its form is clearly not dictated by any physical principle. A modification is therefore proposed in this paper which is globally well-posed, and allows for special natural functions to be stationary solutions. The latter leads to a desirable dynamical behavior from the practical point of view. It also leads to stable pseudo-spectral discretizations with satisfactory properties

from the perspective of image processing. It can also be viewed as a new regularization technique. It differs, however, substantially from other regularization techniques in that it actually makes piecewise constant function become stationary solutions and in that the degree of regularization can be more finely tuned. In particular it does not regularize at any given specific scale.

To simplify the discussion, analytical considerations will be restricted to the one dimensional setting. A representative numerical experiment, however, will be presented also in the natural two dimensional setting. Roughly speaking, the modification proposed consists in replacing the nonlinear term by

$$a_\varepsilon(u) = \frac{1}{1 + [(-A)^{\frac{1-\varepsilon}{2}} u]^2} \quad (1.2)$$

for $\varepsilon \in (0, \frac{1}{2})$ and where A is the Neumann Laplacian. The fractional powers appearing in (1.2) can be defined in various manners depending on the choice of function spaces in which the equation is considered. Since one is interested in denoising while preserving sharp edges, it is clear that a_ε should provide the very same benefits for the kind of large gradients one is interested in preserving. The associated equation

$$u_t - \left(\frac{1}{1 + [(-A)^{1-\varepsilon} u]^2} u_x \right)_x = 0 \quad (1.3)$$

has, however, the advantage of being quasi-linear and of avoiding backward diffusion altogether. The analysis and the numerical experiments performed in this paper therefore also show that backward diffusion is not an essential ingredient in order to preserve sharp edges. For analytical reasons the ideas just presented will be performed on an equivalent formulation of (1.1) leading to an equation of the flavor of (1.2).

2. The Problem

In its one dimensional formulation, the Perona-Malik equation reads

$$\begin{cases} u_t - \left(\frac{1}{1+v_x^2} u_x \right)_x = 0 & \text{in } (0, 1) \text{ for } t > 0, \\ u_x = 0 & \text{at } x = 0, 1 \text{ for } t > 0, \\ u = u_0 & \text{at } t = 0 \text{ in } [0, 1]. \end{cases} \quad (2.1)$$

Introducing $v(x) = \int_0^x u(y) dy$ as a new unknown, it is easily seen that it satisfies

$$\begin{cases} v_t - \frac{1}{1+v_{xx}^2} v_{xx} = 0 & \text{in } (0, 1) \text{ for } t > 0, \\ v(t, 0) = 0, v(t, 1) = \int_0^1 u_0(y) dy & \text{for } t > 0, \\ v(0, \cdot) = \int_0^\cdot u_0(y) dy & \text{in } [0, 1], \end{cases} \quad (2.2)$$

since it is readily verified that the average of u_0 is preserved over time using (2.1). By further defining $w(x) = v(x) - x \int_0^1 u_0(y) dy$, $x \in [0, 1]$, it follows that

$$\begin{cases} w_t - \frac{1}{1+w_{xx}^2} w_{xx} = 0 & \text{in } (0, 1) \text{ for } t > 0, \\ w(t, 0) = 0 = w(t, 1) & \text{for } t > 0, \\ w(0, \cdot) = \int_0^1 u_0(y) dy - (\cdot) \int_0^1 u_0(y) dy & \text{in } [0, 1]. \end{cases} \quad (2.3)$$

Conversely, any solution of (2.2) leads to a solution of (2.1) by setting

$$u(x) = v_x(x), \quad x \in [0, 1].$$

The evolution equation is clearly satisfied whereas for the boundary conditions the following argument is needed. The function

$$\tilde{v}(x) = \int_0^x u(y) dy, \quad x \in [0, 1],$$

satisfies

$$\tilde{v}_t - \frac{1}{1 + \tilde{v}_{xx}^2} \tilde{v}_{xx} = -\frac{u_x(0)}{1 + u_x^2(0)}.$$

Since $\tilde{v} = v$ by $v(0) = 0$ and since v satisfies (2.2), it follows that $\frac{u_x(0)}{1 + u_x^2(0)} = 0$ and therefore $u_x(0) = 0$. Now

$$\int_0^1 u(t, y) dy = v(t, 1) - v(t, 0) = \int_0^1 u_0(y) dy$$

implies that

$$0 = \int_0^1 u_t(y) dy = \frac{u_x(1)}{1 + u_x^2(1)} - \frac{u_x(0)}{1 + u_x^2(0)}$$

and therefore that $u_x(1) = 0$, too. Notice that if u is a piecewise constant function, then v is a continuous piecewise affine function. Thus piecewise affine functions play the same role for (2.3) as piecewise constant functions do for (2.1).

Equation (2.3) is fully nonlinear and clearly presents the same analytical difficulties as the original Perona-Malik equation. The following modification is proposed

$$\begin{cases} u_t - a_\varepsilon(u) Au = 0 & \text{in } (0, 1) \text{ for } t > 0, \\ u(0, \cdot) = u_0 & \text{in } [0, 1], \end{cases} \quad (2.4)$$

for

$$a_\varepsilon(u) = (1 + [(-A)^{1-\varepsilon} u]^2)^{-1}, \quad \varepsilon \in (0, 1/2), \quad (2.5)$$

and where A now denotes the Dirichlet Laplacian. This is perfectly analogous to (1.2). Notice that the intensity of the nonlinearity is barely reduced. It is therefore to be expected that solutions of (2.4) with $\varepsilon > 0$ behave similarly to the solutions of (2.4) with $\varepsilon = 0$ for which the original (1.1) is

recovered, at least at the discrete level. At the continuous level (2.1) is ill-posed and such a claim is not very meaningful. It is therefore likely that (2.4) can provide a viable practical denoising tool while preventing blurring.

Remark 1. It is easily verified that

$$\frac{d}{dt} \int_0^1 v \, dx = 0 \text{ and } \frac{1}{2} \frac{d}{dt} \int_0^1 |v|^2 \, dx = - \int_0^1 \frac{|v_x|^2}{1 + [A^{1-\varepsilon}u]^2} \, dx$$

for $v = u_x$ and a smooth solution u of (2.4).

3. Global Existence of Smooth Solutions

It turns out that (2.4) can be shown to be well-posed in the classical sense as soon as $\varepsilon > 0$. In order to prove this, some notation needs to be introduced. For $\alpha \in [0, 1)$ let

$$C_0^\alpha(0, 1) := \begin{cases} \{u \in C^\alpha([0, 1], \mathbb{R}) \mid u(j) = 0, j = 0, 1\} & \alpha \in (0, 1), \\ C([0, 1], \mathbb{R}) & \alpha = 0, \end{cases}$$

where $C^\alpha([0, 1], \mathbb{R})$ is for $\alpha > 0$ the standard space of Hölder continuous functions endowed with norm

$$\|\cdot\|_\alpha := \|\cdot\|_\infty + [\cdot]_\alpha.$$

The semi-norm $[\cdot]_\alpha$ is given by

$$[u]_\alpha := \sup_{x \neq y} \frac{|u(x) - u(y)|}{|x - y|^\alpha}, \quad u \in C^\alpha([0, 1], \mathbb{R})$$

if $\alpha > 0$. Given $\alpha \in [0, 1)$, the operator A_α is given by

$$\begin{cases} \text{dom } A_\alpha = C_0^{2+\alpha}(0, 1) := \{u \in C^{2+\alpha}(0, 1) \mid u, u_{xx} \in C_0^\alpha(0, 1)\} & \text{for } \alpha > 0 \\ \text{dom } A_0 = C_0^2(0, 1) := \{u \in C^2(0, 1) \mid u(j) = 0, j = 0, 1\} & \text{for } \alpha = 0 \end{cases}$$

and

$$A_\alpha u = u_{xx}, \quad u \in \text{dom}(A_\alpha).$$

Once $\alpha \in [0, 1)$ is fixed, the following simplified notation will be used

$$A := A_\alpha, \quad E_0 := C_0^\alpha(0, 1), \quad E_1 = C_0^{2+\alpha}(0, 1).$$

It follows from [11, Corollary 3.1.21, Corollary 3.1.32, Theorem 3.1.34] that A is a sectorial operator and therefore generates an analytic semi-group $\{e^{tA} \mid t \geq 0\}$ on E_0 . Then its fractional powers $(-A)^\gamma$, $\gamma \in (0, 1)$, can be defined as the inverses of

$$(-A)^{-\gamma} := \frac{1}{\Gamma(\gamma)} \int_0^\infty t^{\gamma-1} e^{tA} \, dt$$

defined on their range, that is, by

$$\text{dom}((-A)^\gamma) = \text{R}((-A)^{-\gamma})^{-1}, \quad (-A)^\gamma = ((-A)^{-\gamma})^{-1}.$$

The domain of $(-A)^\gamma$ might not be an interpolation space between E_1 and E_0 but it satisfies the interpolation inequality

$$\|(-A)^\gamma x\|_{E_0} \leq c \|x\|_{E_0}^{1-\gamma} \|Ax\|_{E_0}^\gamma, \quad x \in \text{dom}(A). \quad (3.1)$$

It can, however, be sandwiched between known interpolation spaces

$$(E_0, E_1)_{\gamma,1} \hookrightarrow D((-A)^\gamma) \hookrightarrow (E_0, E_1)_{\gamma,\infty} \quad (3.2)$$

where, for $\gamma \in (0, 1)$ and $p \in [1, \infty]$, $(E_0, E_1)_{\gamma,p}$ is the standard real interpolation functor. Observe that for $\alpha = 0$ it can be proved that

$$(E_0, E_1)_{\gamma,\infty} = C_0^{2\gamma}(0, 1), \quad \gamma \in (0, 1) \setminus \left\{\frac{1}{2}\right\}.$$

Hölder spaces of the time variable will also be useful. For $\beta \in (0, 1)$, let

$$\mathbb{E}_0 := C^\beta([0, T], E_0), \quad \mathbb{E}_1 := C^{1+\beta}([0, T], E_0) \cap C^\beta([0, T], E_1). \quad (3.3)$$

If $u \in \mathbb{E}_1$, then

$$\frac{1}{1 + [(-A)^{1-\varepsilon}u(t)]^2} A$$

is sectorial for every fixed t . By Hölder maximal regularity (see [11, Proposition 6.1.3]) it follows that any solution of

$$\begin{cases} v_t - \frac{1}{1 + [(-A)^{1-\varepsilon}u]^2} Av = 0 & \text{for } t > 0 \\ v(0) = u_0 \end{cases}$$

satisfies $u \in \mathbb{E}_1$ for any $u_0 \in E_1$ such that $Au_0 \in (E_0, E_1)_{\beta,\infty}$. In order to apply the mentioned theorem, one needs also to take into account the additional facts that

$$[t \mapsto A(t) := \frac{1}{1 + [(-A)^{1-\varepsilon}u(t)]^2} A] \in C^\beta([0, T], \mathcal{L}(E_1, E_0))$$

and

$$\text{dom}(A(t)) = \text{dom}(A(0)), \quad t \in [0, T].$$

It is now possible to prove the following result.

Theorem 1. *Let $u_0 \in E_1$ such that $Au_0 \in (E_0, E_1)_{\beta,\infty}$. Then there exists $T^+(u_0)$ and a unique $u : [0, T^+(u_0)) \rightarrow E_1$ such that $u|_{[0, T]}$ is a solution of (2.4) on the time interval $[0, T]$ for any $0 < T < T^+(u_0)$. Furthermore*

$$u \in C^{1+\beta}([0, T^+(u_0)), E_0) \cap C^\beta([0, T^+(u_0)), E_1)$$

Proof. Let $v \in \mathbb{E}_1$ and define $\Phi(v)$ to be the solution of

$$u_t - \frac{1}{1 + [(-A)^{1-\varepsilon}v]^2} Au = 0, \quad u(0) = u_0.$$

Define $r = 2\|u_0 - \Phi(u_0)\|_{\mathbb{E}_1}$ and let

$$B_r := \{v \in \mathbb{E}_1 \mid \|v - u_0\|_{\mathbb{E}_1} \leq r\}.$$

It follows that

$$\begin{aligned} \|\Phi(v) - u_0\|_{\mathbb{E}_1} &\leq \|\Phi(v) - \Phi(u_0)\|_{\mathbb{E}_1} + \|\Phi(u_0) - u_0\|_{\mathbb{E}_1} = \\ &\quad \left\| [\partial_t - a_\varepsilon(v)A]^{-1}(0, u_0) - [\partial_t - a_\varepsilon(u_0)A]^{-1}(0, u_0) \right\|_{\mathbb{E}_1} + \frac{r}{2} \\ &= \left\| [\partial_t - a_\varepsilon(u_0)A]^{-1} \left\{ 1 - [\partial_t - a_\varepsilon(u_0)A][\partial_t - a_\varepsilon(v)A]^{-1} \right\} (0, u_0) \right\|_{\mathbb{E}_1} + \frac{r}{2} \\ &\leq r \end{aligned}$$

if $T > 0$ is chosen small enough since $v \in B_r$ and $v(0) = u_0$, so that v is uniformly close to u_0 . To see this, consider

$$\begin{aligned} \| [a_\varepsilon(v) - a_\varepsilon(u_0)]A \|_{\mathcal{L}(\mathbb{E}_1, \mathbb{E}_0)} &\leq \| a_\varepsilon(v) - a_\varepsilon(u_0) \|_{\mathcal{L}(\mathbb{E}_0)} \\ &\leq \| (-A)^{1-\varepsilon}(v - u_0) \|_{\mathbb{E}_0} \end{aligned} \quad (3.4)$$

which follows from

$$\left\| \frac{1}{1 + w^2(t)} - \frac{1}{1 + w^2(s)} \right\|_{E_0} \leq \|w(s) - w(t)\|_{E_0}$$

by setting $w = (-A)^{1-\varepsilon}v$ since $v(0) = u_0$ and $a_\varepsilon(u_0)$ are independent of the time variable. To further estimate (3.4), one can use the interpolation inequality (3.1) and

$$v(t) - v(s) = \int_s^t \dot{v}(\tau) d\tau \quad \text{and} \quad \dot{v} \in L_\infty E_0 \quad (3.5)$$

to obtain

$$\begin{aligned} \| (-A)^{1-\varepsilon}[v(t) - u_0] \|_{E_0} &\leq c \|v(t) - u_0\|_{E_1}^{1-\varepsilon} \|v(t) - u_0\|_{E_0}^\varepsilon \\ &\leq crt^{\beta(1-\varepsilon)+\varepsilon}, \quad s, t \leq T, \end{aligned}$$

and

$$\begin{aligned} \| (-A)^{1-\varepsilon}[v(t) - v(s)] \|_{E_0} &\leq c \|v(t) - v(s)\|_{E_1}^{1-\varepsilon} \|v(t) - v(s)\|_{E_0}^\varepsilon \\ &\leq cr|t - s|^{\beta(1-\varepsilon)+\varepsilon}, \quad s, t \leq T. \end{aligned}$$

It follows that

$$\left[(-A)^{1-\varepsilon}(v - u_0) \right]_\beta \leq crT^{(1-\beta)\varepsilon}.$$

and finally that

$$\| [a_\varepsilon(v) - a_\varepsilon(u_0)]A \|_{\mathcal{L}(\mathbb{E}_1, \mathbb{E}_0)} \leq crT^{(1-\beta)\varepsilon}$$

Thus the claimed inequality follows by a simple Neumann series argument made possible by choosing T small enough. Next observe that $\Phi(v_1) - \Phi(v_2)$ solves

$$\begin{cases} [\Phi(v_1) - \Phi(v_2)]_t = a_\varepsilon(v_1)A[\Phi(v_1) - \Phi(v_2)] + (a_\varepsilon(v_1) - a_\varepsilon(v_2))A\Phi(v_2) \\ [\Phi(v_1) - \Phi(v_2)](0) = 0 \end{cases}$$

It follows that

$$\Phi(v_1) - \Phi(v_2) = [\partial_t - a_\varepsilon(v_1)A]^{-1} \left\{ 0, [a_\varepsilon(v_1) - a_\varepsilon(v_2)]A\Phi(v_2) \right\}.$$

Thus

$$\begin{aligned} \|\Phi(v_1) - \Phi(v_2)\|_{\mathbb{E}_1} &\leq c(r) \| [a_\varepsilon(v_1) - a_\varepsilon(v_2)]A\Phi(v_2) \|_{E_0} \\ &\leq c(r) \|A^{1-\varepsilon}[v_1 - v_2]\|_{\mathbb{E}_0} \|\Phi(v_2)\|_{\mathbb{E}_1} \end{aligned}$$

Now, since $v_1 - v_2 \in \mathbb{E}_1$ it follows that

$$\|A^{1-\varepsilon}[v_1 - v_2]\|_{\mathbb{E}_0} \leq c\|v_1 - v_2\|_{\mathbb{E}_1} T^{\varepsilon(1-\beta)}$$

by making use of the interpolation inequality (3.1) and of (3.5) in a perfectly similar way to the calculations used to obtain the self-map property. Thus Banach fixed-point Theorem implies the existence of a unique solution

$$u \in \mathbb{E}_1$$

provided the time interval is chosen short enough. It follows from [11, Proposition 6.1.3] that

$$\dot{u}(t) \in (E_0, E_1)_{\beta, \infty}, \quad t \in (0, T]$$

which gives $Au(T) \in (E_0, E_1)_{\beta, \infty}$. Thus, by using the same argument, the solution can be extended to a larger interval of existence. Repeating this argument indefinitely, a solution is obtained on a maximal interval of existence $[0, T^+(u_0))$ with the stated properties.

Next classical Sobolev spaces are needed

$$W_p^2(0, 1) = \{u \in L_p(0, 1) \mid \partial^j u \in L_p(0, 1) \text{ for } 0 \leq j \leq 2\}$$

for $p \in (0, \infty)$ where the derivatives have of course to be understood in the distributional sense. The simple embedding

$$W_p^s(0, 1) \hookrightarrow C^{s-1/p}(0, 1), \quad sp > 1, \quad (3.6)$$

will be very useful in the proof of the next Lemma.

Lemma 1. *If it can be shown that $u \in L_\infty([0, T^+(u_0)), W_p^2(0, 1))$ for all $p \in (1, \infty)$, then the solution exists globally in time.*

Proof. Observe that

$$\dot{u} = a_\varepsilon(u)\Delta u \in L_\infty([0, T^+(u_0)], L_p(0, 1))$$

follows from the assumption and the form of a_ε . For $s, t \in [0, T^+(u_0)]$, one has

$$\begin{aligned} & \|A^{1-\varepsilon}(u(t) - u(s))\|_{C^{\tilde{\rho}}} \\ & \leq c \|A^{1-\varepsilon}(u(t) - u(s))\|_{W_p^{2\rho}} \leq c \|A^{1-\varepsilon+\rho}(u(t) - u(s))\|_{L_p} \\ & \leq c \|A(u(t) - u(s))\|_{L_p}^{1-\varepsilon+\rho} \left\| \int_s^t \dot{u}(\tau) d\tau \right\|_{L_p}^{\varepsilon-\rho} \leq c |t - s|^{\varepsilon-\rho} \end{aligned}$$

as follows from (3.6) and (3.1). Hereby it needs to be assumed that

$$\tilde{\rho} = 2\rho - \frac{1}{p} > 0 \text{ and } 0 < \rho < \varepsilon.$$

This can always be achieved by choosing p large enough and yields

$$A^{1-\varepsilon}u \in C^{\varepsilon-\rho}([0, T^+(u_0)], C^{\tilde{\rho}}(0, 1)). \quad (3.7)$$

Denote the function space in (3.7) by \mathbb{E}_0 . Let then v be the solution of

$$\dot{v} - a_\varepsilon(u)Av = 0, \quad v(0) = u_0$$

on $[0, T^+(u_0)]$. It satisfies $v \in \mathbb{E}_1$ and one has

$$v|_{[0, T]} = u|_{[0, T]}, \quad T < T^+(u_0)$$

by uniqueness. Since v is uniformly (Hölder) continuous, so must be u . It can therefore be extended as a solution to $[0, T^+(u_0)]$ and as a consequence of Theorem 1 beyond any finite time. The solution is therefore global.

Lemma 2. *Let $u_0 \in C^\infty([0, 1])$ satisfy compatibility conditions to all orders, that is, assume that $u_0 \in \text{dom}((-A)^k)$, $k \in \mathbb{N}$. Then the solution of (2.4) satisfies*

$$u \in C^{1+\beta}([0, T^+(u_0)], C^\infty([0, 1])),$$

for $\beta < \varepsilon$.

Proof. Let u be the solution of (2.4). Then

$$(-A)^{1-\varepsilon}u \in C^\beta([0, T^+(u_0)], C_0^{\alpha+2\beta}(0, 1))$$

since $\beta < \varepsilon$ and u is therefore also a solution of (1.1) in \mathbb{E}_1 for $\alpha + \beta$. By repeating this boot-strapping argument indefinitely one obtains the claim.

Remark 2. Time regularity can also be improved by similar boot-strapping arguments but it will play no role in this paper.

It is now possible to prove the following global regularity results.

Theorem 2. *The maximal solution of (2.4) exists globally.*

Proof. According to Lemma 1 it is enough to show

$$\|Au(t)\|_{W_p^2} \leq c, \quad t \in [0, T^+(u_0)] \text{ for } p \in (0, \infty).$$

By Lemma 2 it follows from (1.1) that

$$\begin{cases} A\dot{u} - A(a_\varepsilon(u)Au) = 0, \\ Au(0) = u_0. \end{cases}$$

Thus $v := Au$ satisfies

$$\begin{cases} \dot{v} - A(a_\varepsilon(u)v) = 0, \\ v(0) = u_0. \end{cases} \quad (3.8)$$

Observe that $a_\varepsilon(u(t))A \cdot$ is, for any fixed time t , formally adjoint to the operator $A[a_\varepsilon(u(t)) \cdot]$. The evolution operator $U_\mathbb{A}(t, \tau)$ generated by $\mathbb{A} = a_\varepsilon(u)A$ on E_0 satisfies

$$\|U_\mathbb{A}(t, \tau)u_0\|_{L_p(0,1)} \leq \|u_0\|_{L_p(0,1)}.$$

This follows from the Trotter-Kato product formula (see [13]) and the fact that the operator

$$c(x)A$$

generates a contraction semigroup on $L_p(0, 1)$ if ellipticity is assumed (cf. [3]). Let $T < T^+(u_0)$ and consider the family of generators $\mathbb{B} = \mathbb{A}(T - t)$, $t \in [0, T]$. Then an easy computation based on

$$\frac{d}{d\tau} U_\mathbb{A}(t, \tau)u_0 = -U_\mathbb{A}(t, \tau)\mathbb{A}(\tau)u_0, \quad u_0 \in \text{dom } \mathbb{A}(0),$$

reveals that

$$U_\mathbb{B}^*(T, T - t)v_0, \quad t \in [0, T],$$

satisfies (3.8) if $U_\mathbb{B}^*$ on $L_{p'}(0, 1)$ is taken to be the evolution operator dual to $U_\mathbb{B}$. Now, since

$$\|U^*(t, \tau)\|_{\mathcal{L}(L_{p'})} = \|U(t, \tau)\|_{\mathcal{L}(L_p)} \leq 1$$

it follows that

$$\|v(t)\|_{L_{p'}} \leq \|v_0\|_{L_{p'}} = \|Au_0\|_{L_{p'}}$$

for any $p \in (1, \infty)$ and therefore

$$\|Au(t)\|_{L_p} \leq c \|u\|_{W_p^2} \leq c \|Au_0\|_{L_p}$$

for all $p \in (1, \infty)$. The proof is thus complete since $T < T^+(u_0)$ is arbitrary and the embedding constant c does not depend on T .

4. Stationary Solutions

Among constant functions, $u \equiv 0$ is clearly a stationary solution of (2.4). It corresponds to a constant solution with value $\int_0^1 u_0(x) dx$ of the original Perona-Malik equation with initial value u_0 . It turns out, however, that other more desirable functions are equilibria of (2.4) as well. Even though the next result remains valid for (2.4), it is formulated in the context of the modified Perona-Malik equation with periodic boundary conditions instead of homogeneous Dirichlet conditions. This allows to simplify a little the argument.

Proposition 1. *Let u be a continuous 1-periodic piecewise affine function. Then*

$$\frac{1}{1 + [(-A)^{1-\varepsilon}u]^2} Au \equiv 0,$$

for A taken to be the realization of ∂_{xx} in the space of Radon measures M_π . The subscript π indicates that the periodic case is considered.

Proof. If u has the properties stated in the proposition, it follows that

$$\partial_{xx}u = \sum_{j=1}^n c_j \delta_{x_j}$$

for some constants $c_j \in \mathbb{R}$ and locations $x_1, \dots, x_n \in [0, 1)$. The claim would therefore follow if it can be proved that

$$\frac{1}{1 + [(-A)^{1-\varepsilon}u]^2}$$

is a continuous function vanishing at x_j , $j = 1, \dots, n$. It is clear that it is enough to consider the case of a function with a single kink. Furthermore, since periodicity is assumed, Poisson's summation formula implies that the singularity in $(-A)^{1-\varepsilon}u$ in $[0, 1)$ is the same as the singularity at the same location for $(-A)^{1-\varepsilon}u$ periodically extended to the real line. By making use of standard localization techniques, it is therefore sufficient to consider a function of the real line with a single kink in the origin and $A = \partial_{xx}$ on the full line. Choose the prototype $u(x) = |x|$. Since

$$(-A)^{1-\varepsilon}u = (-A)^{-\varepsilon} \delta$$

it follows that $\mathcal{F}((-A)^{1-\varepsilon}u) = \frac{1}{|\xi|^{2\varepsilon}}$ and therefore that

$$(-A)^{1-\varepsilon}u = c_\varepsilon \frac{1}{|x|^{1-2\varepsilon}}.$$

for $C_\varepsilon = \sqrt{\frac{2}{\pi}} \Gamma(1-2\varepsilon) \sin(\pi\varepsilon)$. Remember that it has been assumed initially that $\varepsilon \in (0, 1/2)$ to make the nonlinearity strong enough. It follows that, in

the general case, $(-A)^{1-\varepsilon}u$ has integrable singularities at x_j , $j = 1, \dots, n$, and is otherwise smooth by hypo-ellipticity. This shows that

$$\frac{1}{1 + [(-A)^{1-\varepsilon}u]^2}$$

is a continuous function which vanishes exactly at x_j , $j = 1, \dots, n$. It is therefore a well-defined multiplier for $\sum_{j=1}^n c_j \delta_{x_j}$ and one has

$$\frac{1}{1 + [(-A)^{1-\varepsilon}u]^2} Au = 0$$

as claimed.

Remark 3. It should be observed that it is not possible (to the best of our knowledge) to make sense of (1.1) as generating a flow on M_π (or on any of the standard Besov spaces containing Dirac distributions) and so the stationary solutions of the proposition are only formally such. A short computation would even show that they are formally linearly stable. This might help explain the fact that, in numerical calculations of (2.4), it is observed that solution starting close to such a stationary solution tend to stay in its vicinity for a long time before being driven to the trivial steady state. Even more is actually true. Numerical experiments (see Figure 2) show that smooth solutions tend to become piecewise affine at first but are eventually completely smoothed out.

Remark 4. Since the weakened nonlinearity (2.5) does not give rise to forward-backward diffusion for the linearization, global well-posedness can be proved. Its linearization, however, will be closer and closer to the Perona-Malik linearization as ε decreases. As a consequence more and more of its eigenvalues will become negative when linearizing in the presence of large gradients. This is supporting evidence that the numerical benefits of Perona-Malik should not go lost in the modified (2.4).

Remark 5. The new equation is globally well-posed for smooth initial conditions. It is, however, not immediately clear what their large time asymptotic behavior should be. Numerical experiments seem to suggest that any solution will eventually converge to a trivial steady-state. This behavior might, however, be due to numerical diffusion. In the next section a reason will be given which seems to exclude the latter possibility.

Remark 6. It is also observed that the original Perona-Malik equations do not admit piece-wise constant functions as formal stationary points unless an ad-hoc concept of generalized stationary solution is introduced (see [10]) since the multiplication of distributions is in general not well-defined. Its discretization, however, seems to exhibit “almost stability” of such solutions in the sense explained here. This might be an indication that the Perona-Malik equation is regularized by discretization and could explain the success of its implementations in spite of the ill-posedness of its analytical counterpart.

5. Numerical implementation and experiments

Next a numerical discretization of (2.4) is derived in a periodic context and used to perform numerical experiments intended to illustrate and demonstrate the claimed improvements on the classical Perona-Malik equation. The periodic Laplacian A is discretized spectrally by means of the fast Fourier transform F_n

$$A_n = F_n^{-1} A_n F_n \quad (5.1)$$

where $n = 2^m$ denotes the number of grid points used and

$$D_n = 4\pi^2 \operatorname{diag}\left(\left(-\frac{n}{2} + 1\right)^2, \left(-\frac{n}{2} + 2\right)^2, \dots, 0, 1, \dots, \frac{n^2}{4}\right).$$

The time variable is discretized by forward semi-implicit Euler so that

$$u^{k+1} = \left[\operatorname{id}_n - \frac{h_t}{1 + (A_n^{1-\varepsilon} u^k)^2} A_n \right]^{-1} u^k \quad (5.2)$$

where u^k is the spatial n -vector at time $k h_t$ for the time step $h_t > 0$. Observe that, setting $\varepsilon = 0$, the classical Perona-Malik equation is recovered.

The following experiments are presented here. First the evolution of the function

$$u_0(x) := 100x^2(1 - x^2), \quad x \in [0, 1].$$

is considered. Figure 1 depicts the first derivative of the function u^k after 100 time steps of size $h_t = 0.06$ for $m = 8$. The blue curve corresponds to the Perona-Malik solutions and the stair-casing phenomenon is apparent. The red, magenta and cyan curves correspond to solution of the modified equation for $\varepsilon = 0.3, 0.2, 0.1$, respectively. They clearly benefit from all effects of the Perona-Malik equation without leading to stair-casing. Some decrease in contrast is the only price paid. Notice that the black curve depicts the first derivative of the initial value. Comparison with the other curves reveals the de-blurring effect of the equation. It has been proved that continuous piecewise affine functions are steady-states for the modified Perona-Malik equation. There is, however, no mechanism by which a smooth solution can develop a singularity in finite time. The solution therefore feels the presence of these nontrivial steady-states but never leaves the regime where diffusion, slowly but surely, drives it to a trivial steady-state. This is exemplified in Figure 2 where various stages of the evolution of a smooth solution are with initial condition

$$u_0(x) = \sin(2\pi x) + 2 \sin(4\pi x), \quad x \in [0, 1].$$

is depicted. Clearly the convergence towards the trivial steady state might be due to numerical diffusion (see Remark 5). However, Remark 1 provides an indirect way to test the numerics. It follows from Remark 1 that

$$\int_0^1 u_x^2 dx = \int_0^1 (u_0)_x^2 dx - 2 \int_0^t \int_0^1 \frac{u_{xx}^2}{1 + [A^{1-\varepsilon} u]^2} dx d\tau.$$

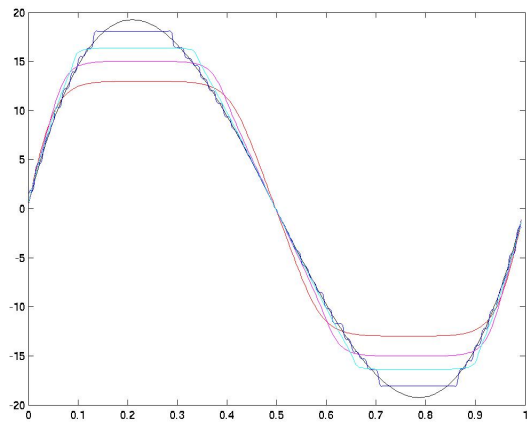


Fig. 1. The gradient of the solution for different values of ε .

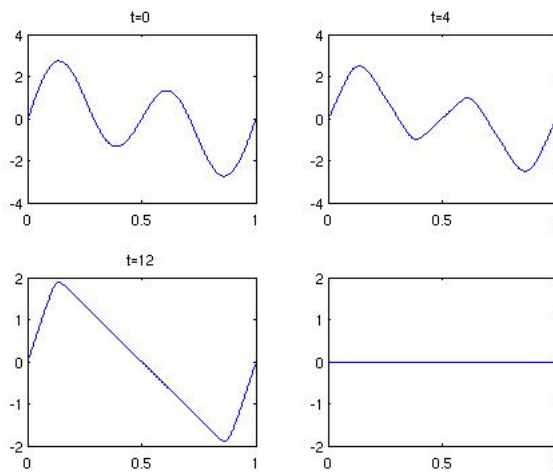


Fig. 2. Tendency to evolve towards or close to piece-wise affine functions.

This conservation relation can be tracked for any smooth solution and, in the particular case considered, the relative numerical deviation observed between the left and right-hand-side of it amounts to a mere 0.2% for a fully converged solution. Scheme (5.2) also preserves the piecewise affine structure of initial values for large integration times. The solution with initial condition

$$u_0(x) = 5 - |10x - 5|, \quad x \in (0, 1),$$

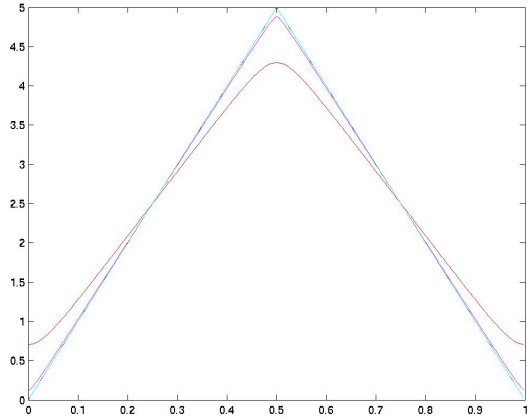


Fig. 3. Behavior close to formally stationary solutions.

is computed for 100 time steps with $h_t = 0.06$ and $m = 8$. The solutions are plotted in Figure 3. The color coding is as in the previous experiment. In spite of the fact that u_0 is a steady-state for any choice of $\varepsilon \in (0, \frac{1}{2})$, numerical dissipation is stronger for larger ε as the relative strength of the non-linearity decreases. The initial value and the solution to $\varepsilon = 0.1$ are indistinguishable in the plot. They differ by 0.2% in the supremum norm. Continuous piecewise linear functions are not steady-states for the original Perona-Malik equation since the non-linearity is not well-defined for such functions. In spite of this its numerical counterpart delivers results comparable to those for small positive ε . Figure 4 shows clearly one of the claimed enhancements of (2.4) over the original Perona-Malik equations. The initial condition (in red)

$$u_0(x) = 5 - |10x - 5| + 0.2 \sin(64\pi x), \quad x \in (0, 1),$$

is evolved to time $t = 2$ (in blue) with $\varepsilon = 0.3$. The new equation can manifestly differentiate between high low contrast gradients and high contrast gradients, which are remarkably well preserved. Observe that the initial oscillatory condition would be left virtually unchanged by the original Perona-Malik equation for the same and longer time ranges. Even though this paper is concerned with a one-dimensional modification of Perona-Malik, equation (2.4) can be considered in a natural two dimensional setting. The qualities of the its one dimensional counterpart considered here do carry over to that case. Figure 5 shows the evolution of a noisy test image every pixel of which has been corrupted by about 15% noise in the gray-scale. For other tests and details of the two-dimensional implementation we refer to [9].

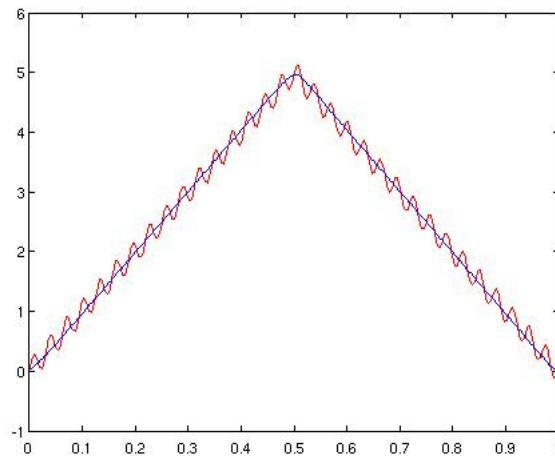


Fig. 4. The effect of (2.4) on high frequency low contrast oscillations. The initial condition (in red) is rapidly evolved to the almost piecewise affine function (in blue).



Fig. 5. The denoising effect obtained for the 2D version of (2.4) with $\varepsilon = 0.6$ and Neumann boundary conditions. The initial condition is Lenna's image corrupted with about 15% salt and pepper noise.

6. Conclusions

A modified Perona-Malik equations has been proposed by strength reduction in the non-linearity via a non-local term. Global well-posedness of the new equation and the fact that piecewise constant functions are steady-states for it are its main analytical advantages. From the practical point of view, the new equation delivers enhanced benefits as compared to Perona-Malik and suppresses known shortcomings associated to it. It provides an easy, effective, and stable tool for image de-noising. These claims are corroborated by numerical experiments.

References

1. L. Alvarez, P.-L. Lions, and J.-M. Morel. Image selective smoothing and edge-detection by non-linear diffusion. ii. *SIAM J. Numer. Anal.*, 29(3):845–866, 1992.
2. H. Amann. Time-Delayed Perona-Malik Problems. *Acta Math. Univ. Comeniana*, LXXVI:1–24, 2006.
3. W. Arendt. Heat kernels. *Internet Seminar 2005/2006*, <https://tulka.mathematik.uni-ulm.de/2005/lectures/internetseminar.ps>.
4. A. Belahmidi. *Equations aux dérivées partielles appliquées à la restauration et à l'aggrandissement des images*. Ph.D. Thesis. Université Paris-Dauphine, Paris, 2003.
5. A. Belahmidi and A. Chambolle. Time-delay regularization of anisotropic diffusion and image processing. *M2AN Math. Model. Numer. Anal.*, 39(2):231–251, 2005.
6. F. Catté, P.-L. Lions, J.-M. Morel, and T. Coll. Image selective smoothing and edge-detection by non-linear diffusion. *SIAM J. Numer. Anal.*, 29(1):182–193, 1992.
7. Y. Chen and P. Bose. On the incorporation of time-delay regularization into curvature-based diffusion. *J. Math. Imaging Vision*, 14(2):149–164, 2001.
8. G. Cottet and M. El Ayyadi. A volterra type model for image processing. *IEEE Trans. Image Processing*, 7:292–303, 1998.
9. P. Guidotti and J. Lambers. A Well-posed Nonlinear Nonlocal Diffusion for Noise Reduction. *Submitted*.
10. S. Kichenassamy. The Perona-Malik paradox. *SIAM J. Appl. Math.*, 57(5):1328–1342, 1997.
11. A. Lunardi. *Analytic Semigroups and Optimal Regularity in Parabolic Problems*. Birkhäuser, Basel, 1995.
12. M. Nitzberg and T. Shiota. Nonlinear image filtering with edge and corner enhancement. *IEEE Trans. Pattern Anal. and Machine Intelligence*, 14:826–833, 1992.
13. A. Pazy. *Semigroups of Linear Operators and Application to Partial Differential Equations*. Springer Verlag, New York, 1983.
14. P. Perona and J. Malik. Scale-space and edge detection using anisotropic diffusion. *IEEE Transactions Pattern Anal. Machine Intelligence*, 12:161–192, 1990.
15. S. Taheri, Q. Tang, and K. Zhang. Young measure solutions and instability of the one-dimensional Perona-Malik equation. *J. Math. Anal. Appl.*, 308:467–490, 2005.
16. K. Zhang. Existence of infinitely many solutions for the one-dimensional Perona-Malik model. *Calc. Var.*, 26(2):171–199, 2006.

103 Multipurpose Science and Technology Building
Department of Mathematics
University of California
Irvine, CA 92697-3875 USA
email: gpatrick@math.uci.edu